Note: This copy is for your personal non-commercial use only. To order presentation-ready copies for distribution to your colleagues or clients, contact us at www.rsna.org/rsnarights.

Apparent Diffusion Coefficient and Beyond: What Diffusion MR Imaging Can Tell Us about Tissue Structure[1]

Denis Le Bihan, MD, PhD

The first images of water diffusion in the human brain were published almost 30 years ago (1). Since then, important methodological and conceptual developments have occurred, and diffusion magnetic resonance (MR) imaging has become a pillar of modern clinical imaging. Diffusion MR imaging has primarily been used to investigate neurologic disorders, especially for the treatment of patients with acute stroke or white matter disorders, but it is also rapidly becoming a standard for body MR imaging, particularly in oncology. What makes diffusion MR imaging so unique is that during their diffusion-driven displacements, water molecules probe tissue structure at a micrometer scale well beyond the usual millimetric MR imaging resolution. The noninvasive observation of the water diffusion–driven displacement distributions thus provides unique clues to the fine structural features and geometric organization of tissues and to changes in those features with physiologic or pathologic states. Diffusion MR images usually come in two forms: diffusion-weighted images and apparent diffusion coefficient (ADC) calculated images.

Diffusion-weighted images are raw images where the signal has been sensitized to diffusion by using strong magnetic field gradient pulses (fast diffusion results in large signal attenuation). The degree of diffusion sensitization is defined by the so-called *b* value (1,2). To save precious acquisition and processing time, clinicians have often limited their diffusion studies to the analysis of such diffusion-weighted images. One must be aware, however, that the content of these images is affected by many parameters other than diffusion, mainly relaxation times T1 and T2. Because these parameters may not have the same behavior as diffusion during different physiologic or pathologic conditions, variations in image intensity may at times be difficult to interpret (3). Hence, whenever possible, quantitative diffusion images should be preferred. In theory, it is possible to obtain pure maps of water diffusion by acquiring two images with different *b* values, according to a simple equation:

$$\mathrm{ADC} = \frac{\ln\left(\frac{S_0}{S_1}\right)}{(b_1 - b_0)},$$

where S_0 and S_1 are the signal intensity obtained with the b_0 and b_1 *b* values, respectively. Calculation can be done on regions of interest or on a voxel-by-voxel basis, thus providing ADC calculated images. This simple equation, however, is accurate (provides the true diffusion coefficient, *D*) only if water diffusion behaves freely, that is, the distribution of diffusion-driven displacements obeys Gaussian law. This is certainly not true in tissues, as we will see in more detail later, but I did suggest in 1986 (1) that one could portray the complex diffusion processes that occur in a biologic tissue on a macroscopic voxel scale by using this simple free diffusion equation as a way to express diffusion MR imaging results in a common frame, while replacing the exact diffusion coefficient, *D*, with an ADC to signify that deviation from true diffusion was expected. In addition, the ADC may also include a component originating from blood flow in random vessels through the intravoxel incoherent motion effect (4). This global ADC was, indeed, intended to "summarize" in some way at voxel (or region-of-interest) level those many hidden physical processes that occur at much smaller scales, given that during typical diffusion times used for diffusion MR imaging, water molecules diffuse on distances on the order of just a few micrometers, encountering or interacting with many other molecules and cellular

Published online
10.1148/radiol.13130420

Radiology 2013; 268:318–322

[1] From NeuroSpin, I²BM/DSV/CEA, Bâtiment 145, Point Courrier 156, 91191 Gif-sur-Yvette, France; and Human Brain Research Center, Graduate School of Medicine, Kyoto University, Kyoto, Japan. Received February 17, 2013; revision requested February 19; revision received February 20; accepted February 21; final version accepted February 21. **Address correspondence to** the author (e-mail: *denis.lebihan@cea.fr*).

Conflicts of interest are listed at the end of this article.

See also the article by Koral et al in this issue.

© RSNA, 2013

components. The ADC allows us to bridge the gap between the two scales somewhat. The averaging smoothing effect resulting from this scaling presumes some homogeneity in the voxel (or the region of interest) and makes a direct physical interpretation of this global parameter somewhat difficult, unless some assumptions can be made. Hence, the reverse problem consisting of retrieving specific information about tissue microscopic features from ADC measurements is somehow ill-posed and yet the object of intense research.

Despite this intrinsic limitation, the ADC concept has been, nonetheless, extremely successful in clinical practice and is still commonly used today, as the following examples beautifully demonstrate. The mother of all diffusion MR imaging applications has certainly been in acute brain stroke, as this application was first described shortly after the discovery that the ADC decreases after the onset of ischemia (5), allowing the rapid diagnosis of acute cerebral ischemia and ultimately the identification of patients who could benefit from thrombolytic therapy in the emergency setting. The reason for this ADC decrease is still unclear, although a link with cell swelling (cytotoxic edema) has been established (6). ADC maps may also allow one to determine the onset of the ischemic event (which is difficult with diffusion-weighted images because of T2 confounding effects [3]) and to predict the clinical outcome, thus, helping to guide therapy (7). Another big application lies in brain white matter disorders. The ADC is anisotropic in white matter (8), as the ADC is smaller perpendicularly to the tracts than along the tracts axes. Here again, the exact mechanism of this anisotropy is not fully understood, although the organization of the axons in parallel bundles within the fibers and the presence of myelin play a crucial role. Diffusion anisotropy is better handled by using the diffusion-tensor imaging framework that Peter Basser and I introduced (9). However, the diffusion tensor (equivalent to a three-dimensional ADC) and its derived diffusion parameters, such as the fractional anisotropy index which is commonly used, rely on the simple free diffusion model of the Equation, as does the ADC. Fractional anisotropy has been found extremely valuable for the assessment of brain maturation in children (10) and in connection disorders, such as in dyslexia (11) and some psychiatric disorders (12). And who has not been astonished by the gorgeous images of brain connections that often make the cover of medical or neuroscience journals and have been highlighted in anatomy textbooks? However, as we will see below, the ADC reaches its limits there, as it cannot allow crossing fibers to be segregated. To mention a recent growing field of application, diffusion MR imaging in the body (13) is becoming extremely popular (sometimes in competition with fluorine 18 fluorodeoxyglucose positron emission tomography) for cancer diagnosis and treatment, as ADC is commonly lower in malignant lesions than in benign lesions and normal surrounding tissues. The "recovery" (increase) of the ADC after chemotherapy has been used to assess the efficacy of chemotherapy well before clinical status improves, allowing physicians to rapidly switch to a more efficient treatment, in the case of apparent poor response (14). Once again, the reason for this ADC decrease, such as cell proliferation, is not straightforward and is sometimes controversial, as illustrated in the article by Koral et al in this issue of *Radiology* (15). But all those examples underline the strength and the power of the ADC concept, despite (or because of) its simplicity. Long live the ADC!

Yet, the full potential of diffusion MR imaging cannot be reached if one limits oneself to the ADC. But, we first have to make sure we really squeeze all the juice out of the ADC and avoid pitfalls. To make sense, the ADC must be obtained from areas where tissue structure is most homogeneous and most representative of underlying tissue structure. When it comes to tumors, the problem is that they are often very heterogeneous. Furthermore, parts of the lesions may contain edema, necrosis, or cystic or hemorrhagic parts, which all tend to increase the ADC and overwhelm the ADC decrease associated with cell proliferation. Hence, proper validation with histologic findings requires registration between diffusion MR images and slices of the anatomic pieces, which is far from trivial. When using biopsy samples, their exact location must precisely correspond to the location of the region of interest used to extract the ADC. This might not be easy, but it is absolutely necessary to draw meaningful conclusions. With large cohorts or groups of patients, localization errors are permitted to some extent, because they will phase out in the statistical average, but validation of diffusion MR imaging data in a small patient population (let's say individual cases), where statistical power remains limited, is more demanding for accuracy, as Koral et al have realized (15). It would then be erroneous to conclude that there is no correlation of the ADC with underlying tissue structure. The correlation may well exist, and even be strong, as shown in some animal studies (14), but could easily be missed. One way to increase chances of not overlooking important parts of a lesion is to refer to the minimum ADC concept. Assuming that the most malignant tumor parts coincide with the lowest ADC, Iima et al (16) have shown that patients with a suspicion of breast cancer based on mammographic findings presenting no part with a minimum ADC below a given threshold within the lesion could be given a diagnosis of low grade ductal carcinoma in situ with 100% specificity; such patients would potentially be spared from useless but aggressive therapies. This is another example that shows that strong conclusion can be made out of the ADC, although details about underlying tissue structure are not obtained. However, if such details are needed, one has to realize that the ADC does not contain all the information that can be extracted from diffusion MR imaging data.

To understand how this hidden information can be revealed, one first has to look at the behavior of the diffusion MR imaging signal. Back in 1985, one would consider oneself lucky with b values as high as 200 sec/mm^2, given the gradient hardware available. When plotted against the b value, the diffusion MR imaging signal would follow a straight line (the slope of which is the ADC), as expected from the Equation. In the 1990s, gradient hardware improvements allowed b values around 1000 sec/mm^2 to be reached. It

was then experimentally established that the water diffusion–sensitized MR imaging signal attenuation in brain tissue (and other tissues as well) as a function of the *b* value could not be well described by a single exponential decay, as the Equation would suggest (see Le Bihan [17] for a review). In other words, when plotted against the *b* value, the diffusion MR imaging signal presents some curvature, which indicates that water diffusion in tissues cannot be modeled by a single Gaussian distribution (18) (Figure). At the somewhat long diffusion times (40–60 msec) imposed by diffusion MR imaging sequences available with clinical MR imagers, the effects of the obstacles (such as cell membranes, fibers, etc) within tissues become predominant, which is certainly responsible for the success diffusion MR imaging has enjoyed, but also makes the curvature difficult to interpret. The first consequence of this curvature is that the ADC calculated from the Equation depends on the choice of *b* values (b_0 and b_1): The ADC calculated from images acquired at low *b* values is larger than that obtained from higher *b* values. For instance, in the brain, while a typical ADC obtained from b_1 = 1000 mm^2/sec and b_0 = 0 mm^2/sec is around 0.8×10^{-3} mm^2/sec, it would decrease to 0.6×10^{-3} mm^2/sec with b_1 = 3000 sec/mm^2 and b_0 = 0 sec/mm^2 and to 0.5×10^{-3} mm^2/sec by using b_1 = 3000 sec/mm^2 and b_0 = 1000 sec/mm^2. Before assessing ADCs, it is therefore mandatory to make and report the appropriate choice of *b* values. The b_1 value of 1000 sec/mm^2, which has been a standard for brain studies, has been determined on statistical grounds to get the best trade-off between the signal attenuation from diffusion and the background noise (19), on the basis of the Equation. But this value may not be ideal if one wishes to grab valuable quantitative information on tissue structure.

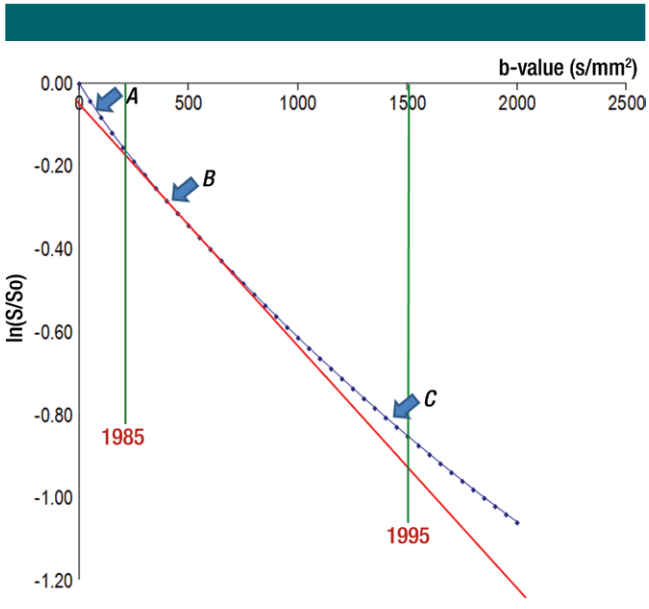

Plot of the diffusion MR imaging signal attenuation (S/S_0) against the *b* value. The plot is straight only with intermediate *b* values (arrow *B*). The slope is then the ADC. At very low *b* values (arrow *A*), the slope is higher, with the inclusion of perfusion (intravoxel incoherent motion effect). At higher *b* values (arrow *C*), the plot gets curved and the slope (ADC) decreases with the *b* value, reflecting its non-Gaussian nature in tissues (hindrance of diffusion by tissue elements, such as cell membranes). Around 1985, only very low *b* values were available. Around 1995, *b* values around 1500 sec/mm^2 became common, while today very high *b* values (5000 sec/mm^2 and higher) can be reached.

Because the ADC in the brain is two to 10 times smaller than free water diffusion in an aqueous solution (which is 3.0 mm^2/sec at 37.5°C), one has to consider the elementary processes hindering diffusion in biologic tissues. High viscosity, macromolecular crowding, and restriction effects have been proposed to explain the water diffusion reduction in the intracellular space. Cell water is not just a structureless space-filling background medium where biologic events occur. In cells, proteins have an especially profound effect on water because of the presence of their charge, which results in protein–water adsorption. Given the high degree of macromolecular packing in cytoplasm and the exchange between water pools, one may consider that a substantial fraction of this adsorbed water contributes to a reduced intracellular diffusion in addition to the presence of obstacles to diffusion (eg, organelles, membranes). Recent studies have pointed out the importance of the hydration process on the structure and function of biologic membranes; in turn, membranes deeply influence water behavior, and the water diffusion coefficient is reduced near the membrane surface (17).

Diffusion is restricted when boundaries in the medium prevent molecules from moving freely (20). When measurement times are very short, most molecules do not have enough time to reach boundaries, so that they behave as if diffusing freely. Once the diffusion time increases, an increasing fraction of molecules strikes the boundaries, and diffusion deviates from free Gaussian behavior. Restricted diffusion effects depend on the shape of the restricting volumes (spherical, cylindrical, parallel walls) and the type of MR imaging experiment, thus there is no unique equation that could describe any configuration. Although variations in the ADC with diffusion times have been reported in the brain (21), no clear restriction behavior has been observed in vivo for water in the brain, except perhaps in dense fiber tracts such as in the corpus callosum, as the diffusion distance seems to increase well beyond cell dimensions with long diffusion times (22). Considering cell membrane

permeability to water is certainly more realistic but adds another level of complication because the mathematical treatment of diffusion in systems partitioned by permeable barriers is far from simple. As for the extracellular space, tortuosity effects are generally considered (23). Tortuosity is a concept that has been widely used in solid porous media studies and more recently in brain diffusion MR imaging. The idea is that, because of the presence of obstacles, such as cells, water molecules must travel longer paths to cover any given distance. In other words, molecules can no longer diffuse in a "straight" way between two locations but must diffuse around cells that are not totally permeable to them. This situation results in an apparent decrease in the diffusion distance covered in a given diffusion time and in the measured ADC.

In summary, cellular components are greatly responsible for the reduced diffusion coefficient in biologic tissues, and there is growing evidence that membranes, even if they are permeable, are likely the main actor that "hinders" the water diffusion process (17). Even if one reduces the diffusion process to membrane interactions, the ADC is expected to depend on both the membrane permeability and its geometry within the tissue, which could have conflicting results on the overall diffusion MR imaging signal. Such considerations have led to some speculations on how the ADC is modulated by cell size (decrease in ADC associated with cell swelling and membrane surface increase, as observed in stroke or neuronal activation [24]), cell density (decrease in ADC associated with the increased membrane content), or cell or membrane orientation (diffusion anisotropy in white matter fibers). But those "explanations" have remained desperately qualitative. Clearly one would like to know much more: amount of cell swelling, or cell density, and so on. To understand better, some physical modeling comes in as a necessity. Simulation work shows that the ADC which is obtained at low b values (typically a few hundred up to 1000 sec/mm^2) mostly reflects the extracellular space unless cells or some cellular elements are strongly elongated along the diffusion measurement direction. The intracellular space remains invisible (and variations of intracellular diffusion cannot be seen), as long as membrane permeability remains normal (that is not particularly high). The variations in ADC according to physiologic or pathologic conditions that have been observed, thus, result from the negative indirect imprint of the cells on the topology of the extracellular space: Cell swelling and cell proliferation tend to "squeeze" the extracellular space, resulting in an increase in tortuosity and a decrease in ADC. However, specificity remains low. For instance, in the presence of two fiber tracts crossing in white matter, water molecules diffusing in the extracellular space may easily switch from the extracellular space surrounding one tract to the other, thereby "losing," at least partially, the orientation feature they acquired along the initial tract. It is now well established that the accuracy of fiber tracking dramatically increases when anisotropic diffusion data are acquired by using high b values (25). With modern gradient hardware, b values up to 4000 sec/mm^2 are no longer out of reach, and recent striking results on brain connectivity have been obtained by using b values as high as 20 000 sec/mm^2 (26). The reason for this race toward high b values is that it gives more access to the intracellular space and membrane interactions: Water molecules sticking inside axons become more visible in the diffusion MR imaging signal, rendering it more representative of the tissue structure than surrounding extracellular water.

The next step is, thus, to characterize the signal behavior at high values. Clearly, the curvature of the diffusion MR imaging signal attenuation can no longer be depicted by using only two b values and one single parameter (the ADC). Instead, efforts are now being made to acquire signals by using an extended range of b values, for instance from 0 to 4000 sec/mm^2. Several models have been introduced to characterize the curvature of the diffusion signal decay. The most popular models are the biexponential model and the kurtosis model. The biexponential model (27) originally assumed the presence of two water pools, one with fast diffusion, the other with slow diffusion (ie, three parameters—the fast and slow volume fractions add up to make 100%). The kurtosis model (28–30) portrays the diffusion signal decay by using three key parameters, the ADC at very low b values and the kurtosis, a parameter that describes the deviation of the signal decay from a single exponential (and diffusion from a free Gaussian process). Those models, though, remain phenomenological: Both fit the signal decay extremely well, but the parameters of the models cannot be directly connected to tissue structure parameters. For instance, the slow and fast pools do not coincide with genuine compartments, certainly not with the intra- and extracellular compartments, as is sometimes found. Exchange effects between the pools (and membrane permeability) have to be taken into account, which is not straightforward. Still, the parameters issued out of those models, for instance the slow volume fraction and the kurtosis, appear as useful markers of the tissue complexity and provide a genuine added value to the ADC in characterizing tissues, for instance in stroke, cancer (31), Alzheimer disease, or schizophrenia (29). One may argue that the acquisition of many b values lengthens the acquisition time, which is not always clinically acceptable. However, with some optimization to minimize the effect of noise, it is possible to reduce the number of b values to a minimum, for instance, only three for the kurtosis model. (The number of necessary b values is the number of parameters in the model plus one, hence two for the ADC.)

We are left with the fact that tissues are extremely complicated, and it is illusory to expect to be able to characterize them in detail with such a limited set of parameters. There is obviously the need for more sophisticated models. If one knows what to look for, it is much easier to find it. By using the example of brain white matter, the tissue can be modeled as a series of parallel cylinders (the axons) where diffusion is restricted, surrounded by extracellular water diffusing freely, although tortuously. This serves as the basis

of the composite hindered and restricted model of diffusion (32) and the AxCaliber method (33): From data collected with multiple *b* values, along several diffusion directions and by using various diffusion times, it is possible to estimate accurately and map the radius of the axons, their distribution, and the axon density within individual fiber bundles. The acquisition time is long, and some errors are possible in fibers that are not well myelinated, as permeability effects are not accounted for in the model, but this is a beautiful example of what can be achieved when appropriate models are used. Other approaches simulate the effect on the diffusion MR imaging signal of random diffusion-driven displacements of water molecules in a realistic, but numeric, model of tissue (tumors, brain cortex, etc). By using these, it then becomes possible to extract features (cell size, shape, density, permeability) out of the signal. Although ADC remains a valid and useful clinical marker, it is clear that more advanced processing of diffusion MR imaging data is necessary if one wants, someday, diffusion MR imaging to become a "virtual biopsy" tool, which remains, so far, its holy grail.

Disclosures of Conflicts of Interest: D.L.B. Financial activities related to the present article: none to disclose. Financial activities not related to the present article: author employed by the French Atomic Energy Commission; institution receives grant from Agence Nationale pour la Recherche. Other relationships: none to disclose.

References

1. Le Bihan D, Breton E, Lallemand D, Grenier P, Cabanis E, Laval-Jeantet M. MR imaging of intravoxel incoherent motions: application to diffusion and perfusion in neurologic disorders. Radiology 1986;161(2):401–407.
2. Le Bihan D, Breton E. In vivo magnetic resonance imaging of diffusion [in French]. C R Acad Sci II 1985;301(15):1109–1112.
3. Burdette JH, Elster AD, Ricci PE. Acute cerebral infarction: quantification of spin-density and T2 shine-through phenomena on diffusion-weighted MR images. Radiology 1999;212(2):333–339.
4. Le Bihan D, Breton E, Lallemand D, Aubin ML, Vignaud J, Laval-Jeantet M. Separation of diffusion and perfusion in intravoxel incoherent motion MR imaging. Radiology 1988;168(2):497–505.
5. Moseley ME, Kucharczyk J, Mintorovitch J, et al. Diffusion-weighted MR imaging of acute stroke: correlation with T2-weighted and magnetic susceptibility-enhanced MR imaging in cats. AJNR Am J Neuroradiol 1990;11(3):423–429.
6. Sotak CH. Nuclear magnetic resonance (NMR) measurement of the apparent diffusion coefficient (ADC) of tissue water and its relationship to cell volume changes in pathological states. Neurochem Int 2004;45(4):569–582.
7. Rosso C, Hevia-Montiel N, Deltour S, et al. Prediction of infarct growth based on apparent diffusion coefficients: penumbral assessment without intravenous contrast material. Radiology 2009;250(1):184–192.
8. Moseley ME, Cohen Y, Kucharczyk J, et al. Diffusion-weighted MR imaging of anisotropic water diffusion in cat central nervous system. Radiology 1990;176(2):439–445.
9. Basser PJ, Mattiello J, LeBihan D. MR diffusion *tensor* spectroscopy and imaging. Biophys J 1994;66(1):259–267.
10. Dubois J, Hertz-Pannier L, Dehaene-Lambertz G, Cointepas Y, Le Bihan D. Assessment of the early organization and maturation of infants' cerebral white matter fiber bundles: a feasibility study using quantitative diffusion tensor imaging and tractography. Neuroimage 2006;30(4):1121–1132.
11. Klingberg T, Hedehus M, Temple E, et al. Microstructure of temporo-parietal white matter as a basis for reading ability: evidence from diffusion tensor magnetic resonance imaging. Neuron 2000;25(2):493–500.
12. Skelly LR, Calhoun V, Meda SA, Kim J, Mathalon DH, Pearlson GD. Diffusion tensor imaging in schizophrenia: relationship to symptoms. Schizophr Res 2008;98(1-3):157–162.
13. Takahara T, Imai Y, Yamashita T, Yasuda S, Nasu S, Van Cauteren M. Diffusion weighted whole body imaging with background body signal suppression (DWIBS): technical improvement using free breathing, STIR and high resolution 3D display. Radiat Med 2004;22(4):275–282.
14. Chenevert TL, Stegman LD, Taylor JM, et al. Diffusion magnetic resonance imaging: an early surrogate marker of therapeutic efficacy in brain tumors. J Natl Cancer Inst 2000;92(24):2029–2036.
15. Koral K, Mathis D, Gimi B, et al. Common pediatric cerebellar tumors: correlation between cell densities and apparent diffusion coefficient metrics. Radiology 2013;268(2):532–537.
16. Iima M, Le Bihan D, Okumura R, et al. Apparent diffusion coefficient as an MR imaging biomarker of low-risk ductal carcinoma in situ: a pilot study. Radiology 2011;260(2):364–372.
17. Le Bihan D. The 'wet mind': water and functional neuroimaging. Phys Med Biol 2007;52(7):R57–R90.
18. Assaf Y, Ben-Bashat D, Chapman J, et al. High b-value q-space analyzed diffusion-weighted MRI: application to multiple sclerosis. Magn Reson Med 2002;47(1):115–126.
19. Xing D, Papadakis NG, Huang CL, Lee VM, Carpenter TA, Hall LD. Optimised diffusion-weighting for measurement of apparent diffusion coefficient (ADC) in human brain. Magn Reson Imaging 1997;15(7):771–784.
20. Tanner JE. Self diffusion of water in frog muscle. Biophys J 1979;28(1):107–116.
21. Assaf Y, Cohen Y. Non-mono-exponential attenuation of water and N-acetyl aspartate signals due to diffusion in brain tissue. J Magn Reson 1998;131(1):69–85.
22. Moonen CT, Pekar J, de Vleeschouwer MH, van Gelderen P, van Zijl PC, DesPres D. Restricted and anisotropic displacement of water in healthy cat brain and in stroke studied by NMR diffusion imaging. Magn Reson Med 1991;19(2):327–332.
23. Nicholson C, Syková E. Extracellular space structure revealed by diffusion analysis. Trends Neurosci 1998;21(5):207–215.
24. Le Bihan D, Urayama S, Aso T, Hanakawa T, Fukuyama H. Direct and fast detection of neuronal activation in the human brain with diffusion MRI. Proc Natl Acad Sci U S A 2006;103(21):8263–8268.
25. Yeh CH, Tournier JD, Cho KH, Lin CP, Calamante F, Connelly A. The effect of finite diffusion gradient pulse duration on fibre orientation estimation in diffusion MRI. Neuroimage 2010;51(2):743–751.
26. Wedeen VJ, Rosene DL, Wang RR, et al. The geometric structure of the brain fiber pathways. Science 2012;335(6076):1628–1634.
27. Niendorf T, Dijkhuizen RM, Norris DG, van Lookeren Campagne M, Nicolay K. Biexponential diffusion attenuation in various states of brain tissue: implications for diffusion-weighted imaging. Magn Reson Med 1996;36(6):847–857.
28. Chabert S, Mecca CC, Le Bihan DJ. Relevance of the information about the diffusion distribution in invo given by kurtosis in q-space imaging [abstr]. In: Proceedings of the Twelfth Meeting of the International Society for Magnetic Resonance in Medicine. Berkeley, Calif: International Society for Magnetic Resonance in Medicine, 2004;1238.
29. Jensen JH, Helpern JA. MRI quantification of non-Gaussian water diffusion by kurtosis analysis. NMR Biomed 2010;23(7):698–710.
30. Jensen JH, Helpern JA, Ramani AL, Lu H, Kaczynski K. Diffusional kurtosis imaging: the quantification of non-gaussian water diffusion by means of magnetic resonance imaging. Magn Reson Med 2005;53(6):1432–1440.
31. Rosenkrantz AB, Sigmund EE, Johnson G, et al. Prostate cancer: feasibility and preliminary experience of a diffusional kurtosis model for detection and assessment of aggressiveness of peripheral zone cancer. Radiology 2012;264(1):126–135.
32. Assaf Y, Freidlin RZ, Rohde GK, Basser PJ. New modeling and experimental framework to characterize hindered and restricted water diffusion in brain white matter. Magn Reson Med 2004;52(5):965–978.
33. Assaf Y, Blumenfeld-Katzir T, Yovel Y, Basser PJ. AxCaliber: a method for measuring axon diameter distribution from diffusion MRI. Magn Reson Med 2008;59(6):1347–1354.